Some Properties of Acoustic Phonons in a Superlattice

Hatsuyoshi KATO *

(Received November 30, 1993)

Abstract

Transmission rate and dispersion relation of phonons in a superlattice were calculated theoretically. The superlattice is assumed to consist of GaAs and AlAs, whose interface is (111) plane. In this calculation, wave vectors of the phonons are restricted within ($\bar{1}10$) plane, and only the SH wave is considered. But incident angles of phonons are not restricted to an angle normal to the (111) interface. At oblique incidence, frequency gaps are found other than at zone boundaries and zone center in the dispersion relation. And the frequency gaps are corresponding to frequencies of dips in the transmission rates.

1. Introduction

Various phonon properties in superlattices have been studied both theoretically and experimentally[1]. In most cases, incidence angles are restricted to normal to interfaces of superlattices. Or the interfaces have even-fold symmetery like (001) plane.

In this paper we considered the case where the interface has three-fold symmetry, i. e. the (111) plane. In this superlattice, incident angles and the reflected angles are not necessarily the same as in the case of interfaces with even-fold symmetries. This causes differences between the incident and reflected angles as will be explained later.

Fig. 1 shows the structure of a superlattice we consider. Unit cell of the superlattice consists of 150-monolayer-AlAs and 60-monolayer-GaAs as shown in Fig. 1 (a). Each monolayer has a thickness of 0.326 nm, i. e. thickness of this unit cell is D = 68.5 nm. The superlattice consists of five unit cells. Substrate is assumed to be GaAs, and detector layer is AlAs as shown in Fig. 1 (b).

In this paper we used the numerical values of the material densities and stiffness coefficients given by S. Adachi[2].

2. Slowness Surface

Both AlAs and GaAs are the cubic crystals. So the slowness surfaces are easy to draw. Fig. 2 (a) shows slowness curves in the ($\bar{1}10$) plane of GaAs. AlAs has the similar slowness curves in the ($\bar{1}10$) plane, but their sizes are smaller than those of GaAs. Fig. 2 (b) shows slowness curves in ($\bar{1}10$) plane, whose left hand part is of AlAs and whose right hand part is of GaAs. The (111) interface is normal to the sheet and separates AlAs slowness curves from GaAs slowness curves. Thick lines in both Fig. 2 (a) and (b) show slowness curves of SH phonons (or pure shear waves), whose polarization vector is perpendicular to the sheet (or parallel to [$\bar{1}10$] direction).

In this paper we concentrate on the SH phonons. The SH phonons can easily be analyzed theoretically. This is because SH phonons do not couple with the other modes in the reflection or transmission processed at the (111) interface as far as the ($\bar{1}10$) sagittal plane is concerned.

In the numerical calculations we used stiffness coefficients as given in the Appendix.

* Lecturer in Physics, Geneneral Education

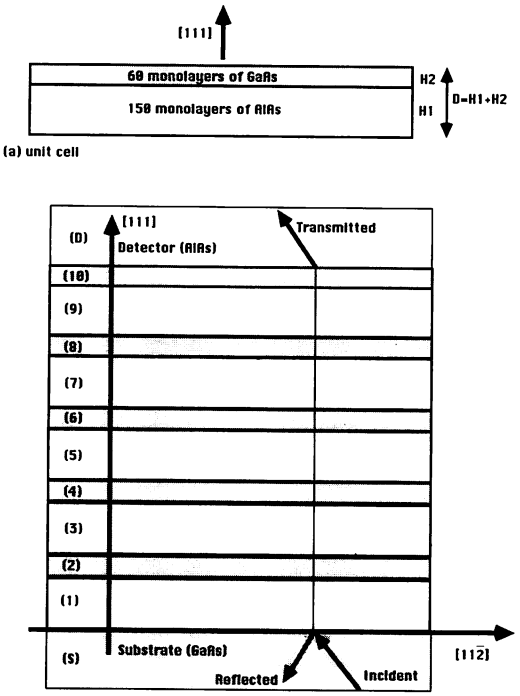

Figure 1

Figure 1 Structure of the superlattice.

(a) A unit cell consists of 60-monolayer-GaAs and 150-monolayer-AlAs, and their thicknesses are H2 = 60 × 0.32639 nm, H1 = 150 × 0.32639 nm respectively. Total thickness becomes D = H1 + H2 = 68.5419 nm.

(b) Substrate is made of GaAs. From this substrate to the interface, incident waves are propagating. And from the interface some parts of incident waves are reflected. Transmitted waves appear in the detector layer, in which no reflected waves do not exist.

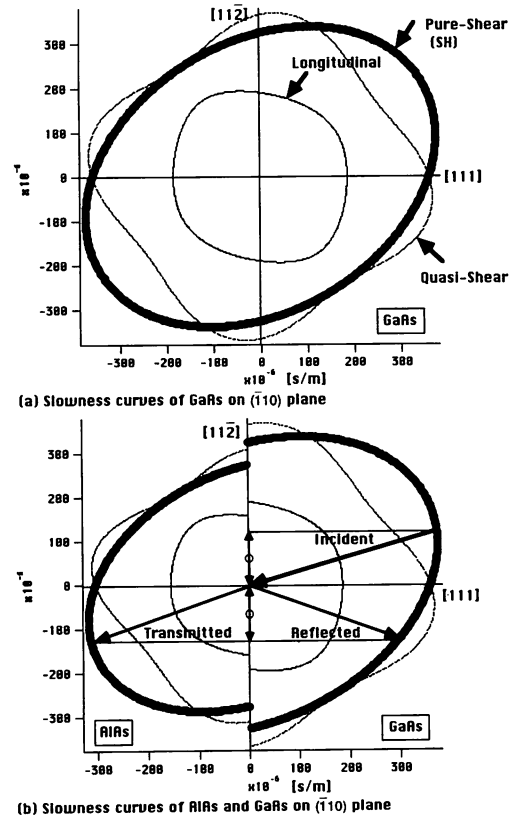

Figure 2

Figure 2 Slowness curves on ($\bar{1}$10) plane.

(a) The slowness curves are shown in a GaAs bulk. Thick oval line is of pure-shear (SH) waves that we are considering. There are another two curves for quasi-shear waves and longitudinal waves.

(b) Slowness curves of AlAs and GaAs are shown in a figure separated by (111) interface. If we consider incident wave propagating from GaAs to AlAs with a certain frequency, we can put a corresponding wave vector on the figure. Because of the conservation law of momentum, reflected wave and transmited wave vectors are easy to be shown as in the figure.

3. Transmission Rate

Fig. 3 shows coordinate system that we use for the calculation of transmission rates. X, Y and Z are the crystal axes of a cubic crystal. The axes x, y and z coincide with $[11\bar{2}]$, $[\bar{1}10]$ and [111], respectively. This coordinate system (x, y, z) is obtained by two consecutive orthogonal transformations from the coordinate system (X, Y, Z). At first we rotate (X, Y, Z) about Z-axis by 45 degrees, and then rotate the system by $\cos^{-1}(1/\sqrt{3})$ radians about y-axis. After these transformations, the stiffness matrix of the cubic crystal in the coordinate system (x, y, z) becomes

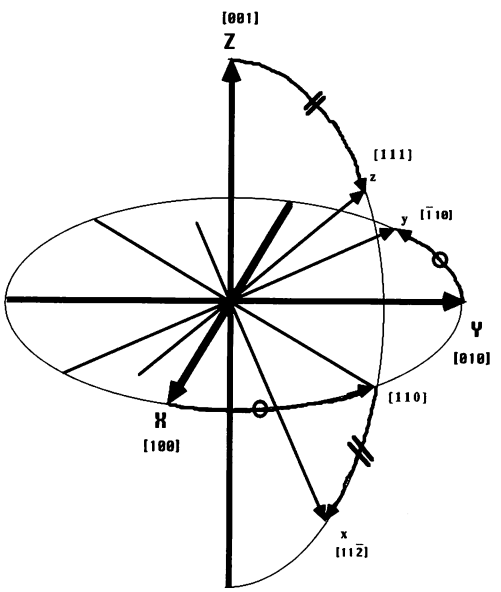

$$[c] = \begin{bmatrix} c_{11} & c_{12} & c_{13} & 0 & c_{15} & 0 \\ c_{21} & c_{22} & c_{23} & 0 & c_{25} & 0 \\ c_{31} & c_{32} & c_{33} & 0 & c_{35} & 0 \\ 0 & 0 & 0 & c_{44} & 0 & c_{46} \\ c_{51} & c_{52} & c_{53} & 0 & c_{55} & 0 \\ 0 & 0 & 0 & c_{64} & 0 & c_{66} \end{bmatrix} \tag{1}$$

Figure 3 Coordinate system for the stiffness matrix.
X, Y, and Z axes are crystal axes of the cubic crystal. The axes x, y, and z are for Eq. (1), whose directions are $[11\bar{2}]$, $[\bar{1}10]$, and [111] respectively.

Each element of this matrix can be expressed by the three independent stiffness coefficients of the cubic crystal. Explicit forms are given in the Appendix. We simply note here that the above matrix [c] is symmertric, i. e. $[c] = [c]^t$.

At first we consider pure shear waves in the bulk[3]. For these waves, the displacement vector of the medium can be expressed as

$$\boldsymbol{u} = \begin{bmatrix} 0 \\ u_y \\ 0 \end{bmatrix}. \tag{2}$$

We also assume that the displacement is a plane wave propagating on the $(\bar{1}10)$ plane and polarized in $[11\bar{2}]$ direction. Thus the nonzero component of Eq. (2) becomes

$$u_y = |u_y| \exp(ik_x x + ik_z z - i\omega t). \tag{3}$$

Equation of motion can be derived from Eq. (1) and Eq. (3) and reduced to

$$c_{66}k_x^2 + c_{44}k_z^2 + 2c_{46}k_x k_z = \rho\omega^2. \tag{4}$$

From this equation we can obtain the slowness curves of SH phonons on the $(\bar{1}10)$ plane. Nonzero elements of the stress tensor derived from Eq. (2) and Eq. (3) are

$$\sigma_{yz} = i(c_{44}k_z + c_{46}k_x)u_y,$$
$$\sigma_{xy} = i(c_{64}k_z + c_{66}k_x)u_y. \tag{5}$$

After some calculations we can express the time averaged energy flux as follows

$$\overline{P_x} = \frac{1}{2}(c_{64}k_z + c_{66}k_x)\,\omega\,|u_y|^2,$$
$$\overline{P_y} = 0,$$
$$\overline{P_z} = \frac{1}{2}(c_{44}k_z + c_{46}k_x)\,\omega\,|u_y|^2. \tag{6}$$

We apply the above results to the superlattice shown in Fig. 1. Superscript (j) on the right shoulders of the quantities means the values in the j-th layer in Fig. 1. In this layer we assume displacements as follows

$$u_x^{(j)} = u_z^{(j)} = 0,$$
$$u_y^{(j)} = A^{(j)}\exp(ik_x x + ik_{z+}^{(j)} z_j - i\omega t) + B^{(j)}\exp(ik_x x - ik_{z-}^{(j)} z_j - i\omega t), \tag{7}$$

where z_j means the z-coordinate measured from the interface between the j-th and (j-1)-th layers. It should be noted that the z-components of wave vectors of incident waves and one of reflected waves are not the same because of the three-fold symmetry of the (111) interface, but the x-components of the wave vectors are the same because of the conservation of momentum or the translational symmetry in the x direction. Non-zero elements of the stress tensor are

$$\sigma_{yz}^{(j)} = i\alpha^{(j)}A^{(j)}\exp(ik_x x + ik_{z+}^{(j)} z_j - i\omega t) + i\beta^{(j)}B^{(j)}\exp(ik_x x - ik_{z-}^{(j)} z_j - i\omega t),$$
$$\sigma_{xy}^{(j)} = i\gamma^{(j)}A^{(j)}\exp(ik_x x + ik_{z+}^{(j)} z_j - i\omega t) + i\delta^{(j)}B^{(j)}\exp(ik_x x - ik_{z-}^{(j)} z_j - i\omega t), \tag{8}$$

where

$$\alpha^{(j)} = c_{44}^{(j)}k_{z+}^{(j)} + c_{46}^{(j)}k_x,$$
$$\beta^{(j)} = -c_{44}^{(j)}k_{z-}^{(j)} + c_{46}^{(j)}k_x,$$
$$\gamma^{(j)} = c_{64}^{(j)}k_{z+}^{(j)} + c_{66}^{(j)}k_x,$$
$$\delta^{(j)} = -c_{64}^{(j)}k_{z-}^{(j)} + c_{66}^{(j)}k_x. \tag{9}$$

Using the boundary condition that the displacement and stress at each interface of j-th and (j + 1)-th layer must be the same, we can get the following matrix expression for the amplitudes in Eq. (7) and Eq. (8):

$$\begin{bmatrix} A^{(j+1)} \\ B^{(j+1)} \end{bmatrix} = [M^{(j+1)}(0)]^{-1} M^{(j)}(H_j) \begin{bmatrix} A^{(j)} \\ B^{(j)} \end{bmatrix}, \tag{10}$$

where

$$M^{(j)}(z_j) = \begin{bmatrix} \exp(ik_{z+}^{(j)} z_j) & \exp(-ik_{z-}^{(j)} z_j) \\ i\alpha^{(j)}\exp(ik_{z+}^{(j)} z_j) & i\beta^{(j)}\exp(-ik_{z-}^{(j)} z_j) \end{bmatrix}. \tag{11}$$

With repetition of the above calculation we can get relation between amplitudes in the substrate and in the detector layer:

$$\begin{bmatrix} A^{(D)} \\ B^{(D)} \end{bmatrix} = [M^{(D)}(0)]^{-1} T^5 M^{(S)}(0) \begin{bmatrix} A^{(S)} \\ B^{(S)} \end{bmatrix}, \tag{12}$$

where

$$T = T^{(2)}T^{(1)},$$

and

$$T^{(j)} = M^{(j)}(H_j)[M^{(j)}(0)]^{-1}. \tag{13}$$

The amplitude $B^{(D)}$ of the reflected wave should vanish in the detector layer[1]. With this condition we can calculate the transmission rates of the SH phonons from the substrate to the detector layer as

$$\frac{\overline{P_z^{(D)}}}{\overline{P_{z+}^{(S)}}} = \frac{\alpha^{(D)}}{\alpha^{(S)}}|F_t|^2, \tag{14}$$

where

$$F_t = \frac{A^{(D)}}{A^{(S)}}. \tag{15}$$

Eq. (15) can be derived from the 2 × 2 matrix in the right hand side of Eq. (12). In Eq. (14), $P_{z+}^{(S)}$ is a ener-

gy flux of the incident waves in the substrate, and $\overline{P_z^{(D)}}$ is one of the transmitted waves in the detector layer. In deriving the above formulae we assume that the phonons are incoherent. Results of numerical calculation are shown in Fig. 4.

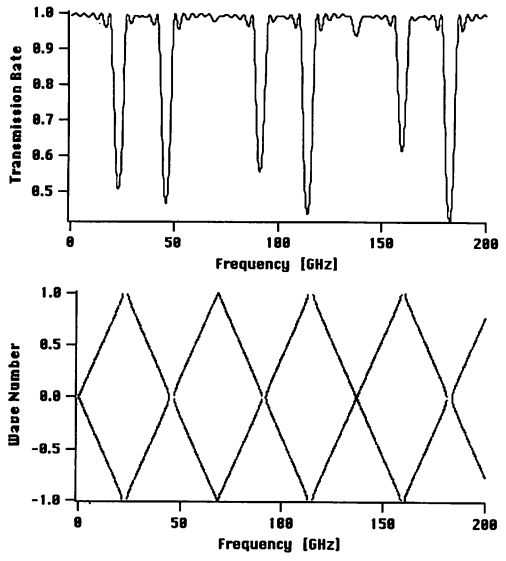

Figure 4 (a) Normal Incidence to the (111) Interface.

Figure 4 Transmission rates and dispersion relations for certain angles of incident wave vectors. Crystal wave numbers of the dispersion relations are normalized by π / D.

(a) Normal incidence to the (111) interface. Frequencies of dips in the transmission rate are corresponding to frequency gaps of the dispersion relation. Each frequency gap is at a zone center or at zone boundaries.

(b) Oblique incidence by 36 degrees from [111] to [001] as shown in figure 2 (b). Arrows in the dispersion relation show the frequency gaps. These gaps are not in the zone center or at zone boundaries as in figure (a). But their frequencies are corresponding to the frequencies of dips in the transmission rate.

(c) Oblique incidence like in the figure (b) is shown. Incident angle is 36 degrees as in figure (b), but its declined direction is opposite, i. e. from [111] direction to [110]. Because of the anisotropy in the (1$\bar{1}$0) plane, transmission rate and dispersion relation are quite different from the figure (b).

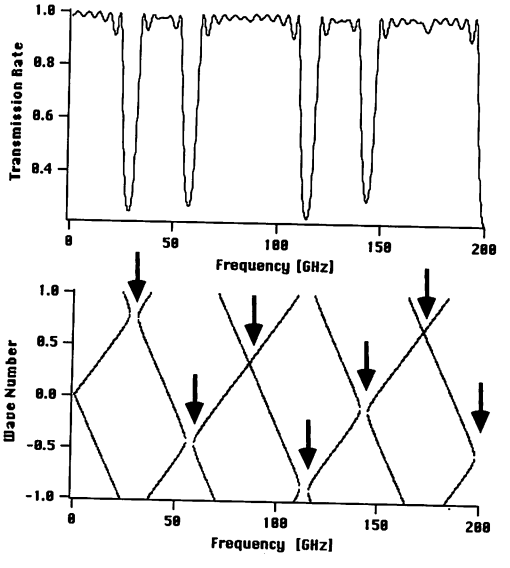

Figure 4 (b) Oblique Incidence by 36 degrees from [111] to [001]

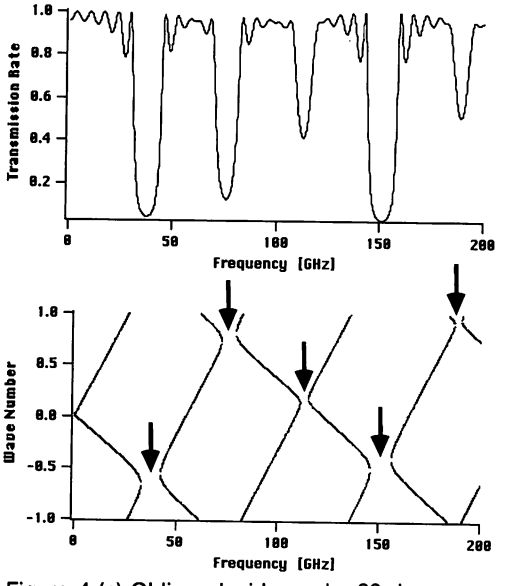

Figure 4 (c) Oblique Incidence by 36 degrees from [111] to [110]

4. Dispersion Relation

Making use of Eq. (13) we can calculate the dispersion relation of the SH phonons on the $(\bar{1}10)$ plane[1]. We define matrix T from a product of the matrices $T^{(j)}$'s for AlAs and GaAs. We use superscript (I) for AlAs and (II) for GaAs, i. e.

$$T = T^{(II)}\, T^{(I)}. \tag{16}$$

If we give a frequency and an incident angle of phonons, the matrix T is determined. The crystal wave number q is then obtained from two eigenvalues of the matrix T. Thus, all we have to do is to solve the characteristic equation:

$$\det [T - \chi E] = 0, \tag{17}$$

where

$$\chi \equiv \exp (iq\, D), \tag{18}$$

and E is a 2×2 unit matrix. Results of numerical calculation are shown also in Fig. 4 together with the transmission rate.

We should note here that determinant of T is not unity, i. e.

$$\det [T] = \exp [i\, (k_{z+}^{(II)} - k_{z-}^{(II)})\, H_{II}] \exp [i\, (k_{z+}^{(I)} - k_{z-}^{(I)})\, H_I]. \tag{19}$$

In this case, $1 / \chi$ is not an eigenvalue of Eq. (17) even if χ is an eigenvalue of the 2×2 matrix T. (This case does happen if the interfaces of a superlattice has even-fold symmetry.) This stems from the difference of the z-components of incident and reflected wave vectors.

5. Discussion and Conclusion

From the slowness curves in Fig. 2, we see that the reflection causes ST to FT mode conversion for the pure shear waves in $(\bar{1}10)$ plane from the (111) interface. As shown in Fig. 4 the dispersion relation has frequency gaps inside the folded zone, and at these gaps the transmission rate has sharp dips. These results stems from the three-fold symmetry of the superlattice we study.

Fig. 2 shows that there exist two phonon modes other than the pure shear wave we are considering. One is the longitudinal pressure wave and the other one is the quasi-shear wave. We have to consider these modes in detail and obtain observable phonon characteristics. A expected feature can be seen in the transmission rate and the dispersion relation of the SH phonons we have derived. We expect similar results are obtained for those two modes.

Appendix

There are general expressions for slowness surfaces for cubic crystals[4]. But these expressions have singularity not convenient to numerical calculations. So we have used stiffness coefficients in the rotated coordinate system given in Eq. (1). We use those results to calculate slowness curves in Fig. 2.

Each element of Eq. (1) can be expressed in three independent elements of stiffness matrix for cubic crystals. We express these three elements by a, b, and c which represent c_{11}, c_{12}, c_{44}, respectively in the usual crystal coordinate system, then the elements of Eq. (1) become as follows. In the following formulae we put

$$Q \equiv \tan^{-1} \frac{1}{\sqrt{2}}\ .$$

$$c_{11} = b \sin^2 Q + c \sin^2 2Q + \cos^2 Q \{ a \cos^2 Q + b \sin^2 Q \} + \frac{a-b+2c}{2} \sin^4 Q$$

$$c_{12} = \frac{a-b-2c}{2} \sin^2 Q + b$$

$$c_{13} = -c \sin^2 2Q + \cos^2 Q \left\{ \frac{3a-b+2c}{2} \sin^2 Q + b \right\} + b \sin^4 Q$$

$$c_{14} = 0$$

$$c_{15} = \sin 2Q \frac{a-b-2c}{4} (3 \sin^2 Q - 2)$$

$$c_{16} = 0$$

$$c_{21} = c_{12}$$

$$c_{22} = \frac{a+b+2c}{2}$$

$$c_{23} = \frac{a-b-2c}{2} \cos^2 Q + b$$

$$c_{24} = 0$$

$$c_{25} = \frac{a-b-2c}{4} \sin 2Q$$

$$c_{26} = 0$$

$$c_{31} = c_{13}$$

$$c_{32} = c_{23}$$

$$c_{33} = a \left(\frac{1}{2} \cos^4 Q + \sin^4 Q \right) + \frac{b+2c}{2} (\cos^4 Q + \sin^2 2Q)$$

$$c_{34} = 0$$

$$c_{35} = \sin 2Q \frac{a-b-2c}{4} (1 - 3 \sin^2 Q)$$

$$c_{36} = 0$$

$$c_{41} = c_{42} = c_{43} = 0$$

$$c_{44} = \frac{a-b-2c}{2} \cos^2 Q + c$$

$$c_{45} = 0$$

$$c_{46} = \frac{a-b-2c}{4} \sin 2Q$$

$$c_{51} = c_{15}$$

$$c_{52} = c_{25}$$

$$c_{53} = c_{35}$$

$$c_{54} = 0$$

$$c_{55} = c + \frac{3}{8} (a - b - 2c) \sin^2 2Q$$

$$c_{56} = 0$$

$$c_{61} = c_{62} = c_{63} = 0$$

$$c_{64} = c_{46}$$

$$c_{65} = 0$$

$$c_{66} = \frac{a-b-2c}{2} \sin^2 Q + c$$

If we rotate the z-axis about the y-axis by larger than μ radians in [110] direction in Fig. 3, we can get stiffness from the above formulae by the substitution

$$Q \equiv \tan^{-1} \frac{1}{\sqrt{2}} - \mu .$$

References

1) S. Tamura, D. C. Hurley, and J. P. Wolfe, Phys. Rev. B, vol. 38, No. 2, 1427 (1988)
2) Sadao Adachi, J. Appl. Phys. vol. 58 (3), R1 (1985)
3) B. A. Auld, *2nd ed. Acoustic Fields and Waves in Solids vol. I, II,* Robert E. Krieger Publishing Company, Malabar, Florida, 1990
4) A. G. Every, Phys. Rev. Lett., vol. 42, No. 16, 1065 (1979)